MENU 2007
11th International Conference
on Meson-Nucleon Physics and
the Structure of the Nucleon
September10-14, 2007
IKP, Forschungzentrum Jülich, Germany

THE PHYSICS PROGRAM AT MAMI-C

Patrick Achenbach
Institut für Kernphysik
Johannes Gutenberg-Universität
J.-J.-Becher-Weg 45
D-55099 Mainz, Germany
Email: patrick@kph.uni-mainz.de

Abstract

In February 2007, the fourth stage of the Mainz Microtron, MAMI-C, started operations with a first experiment. The new Harmonic Double-Sided Microtron delivers an electron beam with energies up to 1.5 GeV while preserving the excellent beam quality of the previous stages. The experimental program at MAMI is focused on studies of the hadron structure in the domain of non-perturbative QCD. In this paper, a few prominent selections of the extensive physics program at MAMI-C will be presented.

1 The new 1.5 GeV Harmonic Double-Sided Microtron as the Fourth Stage of MAMI

The Mainz Microtron MAMI is a unique facility in Europe to study the hadron structure with the electromagnetic probe at small momentum transfers. MAMI comprises a cascade of three race-track microtrons (RTM), delivering since 1991 a high-quality 855 MeV, 100 μA cw-electron beam, which was energy upgraded by a fourth stage, MAMI-C, in recent years. Realizing the fourth stage as another RTM was evidently impossible: the two 180°-bending magnets would have had a weight of approx. 2×2000 tons for an end-point energy of 1.5 GeV. However, for the next higher polytron configuration, the Double-Sided Microtron (DSM), this weight is reduced by a factor of four. By operating at 4.90 GHz, the first harmonic of the fundamental 2.45 GHz radio-frequency (rf), the necessary coherent energy gain per turn for the two normal conducting linacs is reduced to get a moderate power consumption [1]. For achieving a simple transverse optics the strong vertical fringe field defocusing of the four 90°-bending magnets is compensated by a clam-shell field geometry. In this configuration uncritical longitudinal beam

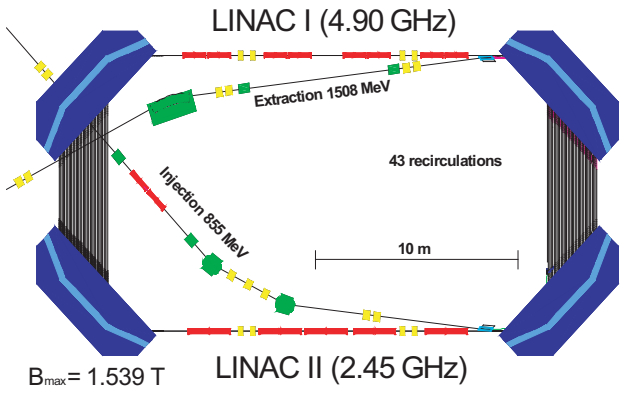

Figure 1: Scheme of the Harmonic Double-Sided Microtron for MAMI- C [2].

dynamics is achieved by operating one of the two linacs at the fundamental rf. The acceleration by two different rf in the Harmonic Double-Sided Microtron (HDSM) is possible because in one of its linacs only every second 4.90 GHz-bucket is occupied [2]. A scheme for the HDSM is given in Fig. 1.

The commissioning of the HDSM started in autumn 2006 with the first full turn through the HDSM. The acceleration along the full 43 recirculations was first operational at the end of 2006, and since February 2007 MAMI-C is delivering a 1.5 GeV high power beam of polarized electrons to the experimental areas.

2 Selection A: Polarized η Electroproduction

The electromagnetic production of η mesons is a selective probe to study the resonance structure of the nucleon. The polarized target asymmetry was measured in Bonn at the PHOENICS experiment [3]. This measurement showed a surprising angular structure, which cannot be described by the existing phenomenological models. A detailed model-independent study [4] showed that one possibility to describe these data is to include a strong phase shift between s- and d-waves.

A measurement of two helicity-dependent polarizations and one helicity-independent polarization in η electroproduction on the proton was performed at the three spectrometer set-up of the A1 collaboration [5]. At $Q^2 = 0.1\,\mathrm{GeV}^2/c^2$ the kinematics of the experiment was chosen for an invariant mass W of the $D_{13}(1520)$ resonance. Neglecting longitudinal multipoles and their interferences the helicity-independent polarizations are dominated by

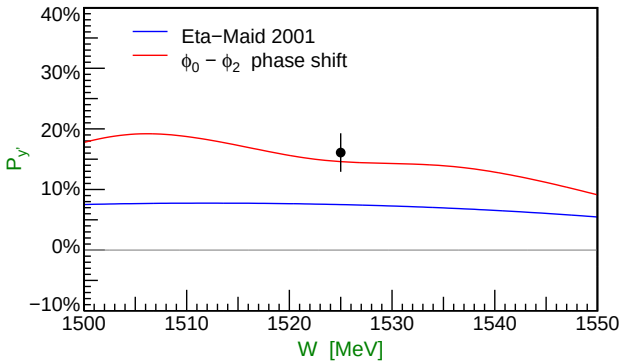

Figure 2: Recoil polarization observable $P_{y'}$ as a function of the c.m. energy W at $\theta = 120°$, $Q^2 = 0.1\,\mathrm{GeV}^2/c^2$, and $\epsilon = 0.718$ from Ref. [5]. The solid line shows the prediction of Eta-MAID [6], the dashed line shows the same model prediction with the energy dependent phase shift of Ref. [4].

the structure functions $R_T^{y'0} \approx \sin\theta\,\Im\left\{E_{0+}^*(3\cos\theta(E_{2-} - 3M_{2-}) - 2M_{1-})\right\}$ and ${}^cR_{TT}^{y'0} \approx 3\sin\theta\cos\theta\,\Im\left\{E_{0+}^*\,(E_{2-} + M_{2-})\right\}$. Thus, the interference with E_{0+} amplifies the sensitivity to the d-wave multipoles E_{2-} and M_{2-}. In particular, ${}^cR_{TT}^{y'0}$ is proportional to the sine of the phase difference between E_{0+} and $E_{2-} + M_{2-}$.

The measured double polarization observables $P_{x'}^h$ and $P_{z'}^h$, dominated by $|E_{0+}|^2$, are well described by the Eta-MAID model. The measured single polarization observable $P_{y'}$ disagrees with the model, see Fig. 2 (solid line). However, if a strong phase change between E_{0+} and $E_{2-} + M_{2-}$, as discussed in Ref. [4], is applied, the data point is in good agreement with the model. Such a strong phase change is not easy to achieve if one assumes a standard Breit-Wigner behavior for the $S_{11}(1535)$ resonance.

3 Selection B: Physics with the Photon Beam

In order to deal with the MAMI-C end-point energy increase, the photon tagging system has been extended and refurbished. The Crystal Ball detector, a photon spectrometer consisting of 672 NaI crystals, has been installed at the photon beam-line in recent years. It is now being used regularly with an inner detector for tracking and the forward photon spectrometer TAPS for a 4π angular coverage, shown in Fig. 3. A new data acquisition system with high-rate performance is in operation and has successfully taken high statistics data [7]. Further, a new frozen spin target of liquid ${}^1\vec{\mathrm{H}}$ and ${}^2\vec{\mathrm{H}}$ is now

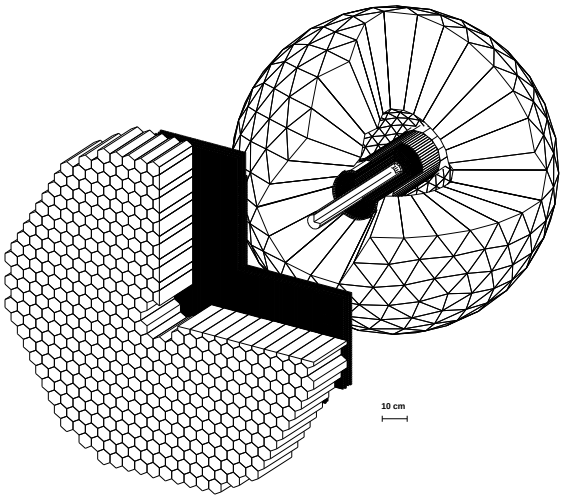

Figure 3: The Crystal Ball detector with the inner tracker and TAPS as forward wall [7].

being commissioned, with the cryostat temperature of 70 mK first reached in June 2007. This target, in particular, provides a unique opportunity to measure the partial contributions to the GDH sum rule on a neutron target. An incomplete list of several topics being addressed by this instrumentation is given here, details can be found in Ref. [1]:

Chiral perturbation theory has been successfully applied to pion photoproduction at threshold. Especially extensions to three flavors urgently require precision data for kaon production processes. Experiments will focus in particular on the following topics: tests of chiral perturbation theory with $\gamma p \to \pi^0 p$ and $\gamma n \to \pi^0 n$; photoinduced kaon production processes close to thresholds; $\gamma p \to \eta' p$ at threshold; and low energy constants of baryon chiral perturbation theory with dispersion analysis of pion electroproduction.

A deeper understanding of the nature of resonances requires a reliable determination not only of the mass spectrum but also of coupling constants and decay vertexes. An essential prerequisite is the exploration of polarization degrees in photoinduced meson production: exploration of the Roper resonance $P_{11}(1440)$ in $\vec{\gamma}\vec{p} \to \pi^0 p$; $S_{11}(1535)$ and $D_{13}(1520)$ in the target asymmetry for the $\gamma p \to \eta p$ reaction; the role of the $D_{15}(1675)$ and $P_{11}(1710)$ in η photoproduction on the neutron; magnetic moment of the $S_{11}(1535)$ in $\gamma p \to \eta p \gamma'$;

and properties of the $S_{11}(1535)$ and $D_{33}(1700)$ resonances in the $\gamma p \to \eta\pi^0 p$ reaction.

The dominant hadronic decay modes $\eta, \eta' \to 3\pi$ only occur due to the isospin violating quark mass difference $m_u - m_d$ or small electromagnetic effects. A systematic study of such decays offers an alternative way to study symmetries and symmetry breaking patterns in strong interactions. Experiments will concentrate on the main neutral decay channels of η and η' mesons: $\pi\pi$ and $\pi\eta$ interactions by a Dalitz plot analysis of the $\eta \to 3\pi^0$, $\eta' \to 3\pi^0$ and $\eta' \to \eta\pi^0\pi^0$ decays; cusp at the opening of the $\pi^0\pi^0 \to \pi^+\pi^-$ threshold in $\eta' \to \eta\pi^0\pi^0$ and the $\pi\pi$ scattering length; and anomalous η decays and corrections to the Wess-Zumino-Witten action at $O(p^6)$.

4 Selection C: Spectrometry of Kaons

The spectrometer facility in Mainz consists of three vertically deflecting magnetic spectrometers freely rotable around a common pivot. However, the detection of kaons under small scattering angles is not possible with these spectrometers due to the short lifetime of the kaons ($c\tau_K = 3.71\,\mathrm{m}$) and the long flight path (close to 10 m for spectrometer C), and their limited forward acceptance (5.6 msr and 28 msr). Therefore, reaction products with strangeness under forward scattering angles need to be analyzed with a short-orbit spectrometer.

KAOS/A1 is a very compact magnetic dipole spectrometer with a large acceptance in solid angle, $\Omega \approx 50\,\mathrm{msr}$, and in momentum, $p_{max}/p_{min} \approx 2$, making it suitable especially for the detection of kaons. It was used (as KaoS) in heavy ion induced experiments at the SIS facility (GSI) in the 1990s [8]. For the use at the spectrometer facility in Mainz a new, flexible concept for a support structure was needed, based on a compact, mobile and adjustable platform on hydraulic positioning feet. The platform with the spectrometer is being moved from a installation position to a measurement position via a displacement system of hydraulic pressure cylinders on skid-tracks. A return to its parking position enables the complete coverage of the forward angle region through the vertical spectrometers. The mechanical parts for this complex installation were designed and constructed from 2003–6.

In November 2007 a first coincidence experiment was performed with KAOS/A1 as hadron arm and spectrometer B as electron arm. However, a series of measurements, among them the detection of hypernuclei at very forward angles, will be made possible only by the use of KAOS/A1 as a double spectrometer. Experiments will be performed close to production thresholds leaving very small center-of-mass energies to the reaction particles, so that

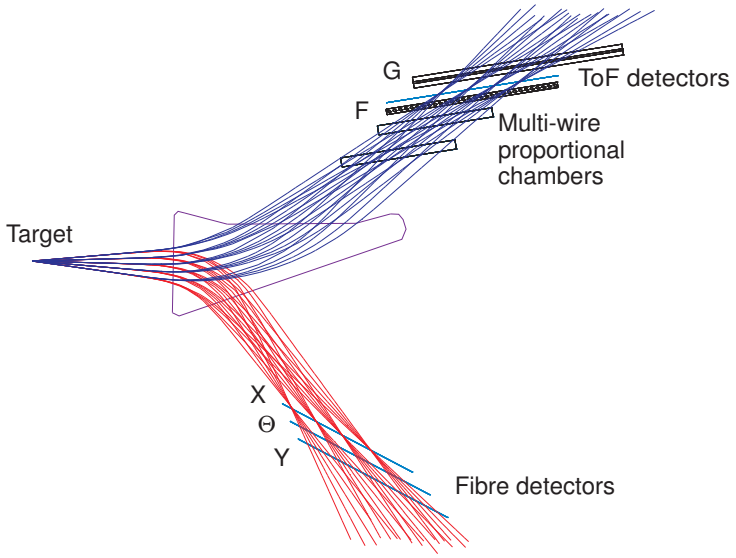

Figure 4: For the operation of KAOS/A1 as a double spectrometer trajectories of positively (p = 600, 675, 750, 825 MeV/c) and negatively charged (p = 280, 310, 340, 370 MeV/c) particles were simulated. The position of the focal planes with respect to the pole shoe contour is indicated.

those are moving with approximate center-of-mass velocity. The operation of KAOS/A1 as a double spectrometer benefits of the accessibility of both pole face edges. Simulated trajectories of positively and negatively charged particles of four different momenta are shown in Fig. 4. The developments for the instrumentation of the electron arm are well advanced [9].

5 Selection D: ϕ Meson Electroproduction

The question of how properties of hadrons change once they are embedded in nuclei is of fundamental interest. In particular the ϕ meson provides an appealing probe for this field. Its properties in nuclei are intimately connected to the way kaons and anti-kaons are modified in a nuclear medium [11, 12] and may provide information on the in-medium strange-quark condensate $\langle s\bar{s}\rangle$ [13]. ϕ mesons decaying within nuclei can be studied via the e^+e^- as well as the K^+K^- decay channels. Electrons practically do not interact with the nuclear medium while the kaons interact strongly with the nucleus themselves. Thus, studying ϕ decays under well defined conditions may allow us to disentangle medium properties of the ϕ meson on one hand and properties of kaons propagating within a nucleus on the other hand. Concerning the exper-

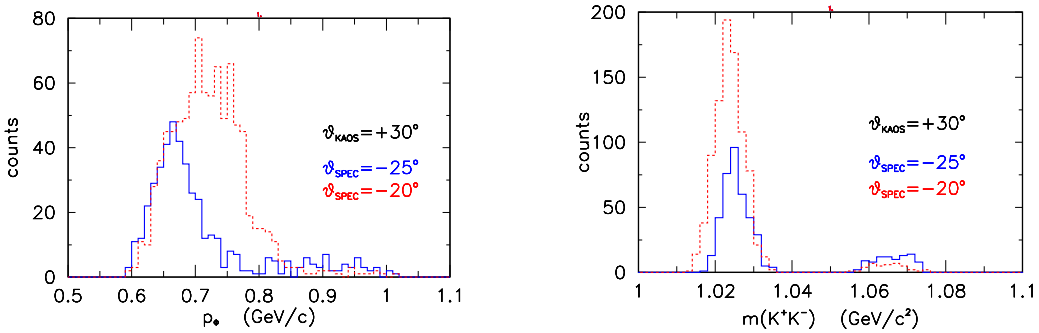

Figure 5: Left: momentum distribution of ϕ mesons reconstructed via the K^+K^- decay channel. KAOS/A1 is positioned at an in-plane angle of $\vartheta = 30°$ and spectrometer C placed at $-20°$ (dashed histogram) or $-25°$ (solid histogram). Right: reconstructed K^+K^- invariant mass.

imental side, the natural width of the ϕ is rather narrow ($\Gamma = 4.26\,\mathrm{MeV}/c^2$) and it is not masked by other neighboring resonances. Consequently, even the small medium modifications of typically few percent expected for the ϕ mass at normal nuclear density [12, 14, 15] may be observable.

Although the maximum beam energy of MAMI-C does not allow the direct associated production of K^+K^- pairs on an individual nucleon at rest, the study of the coherent production of K^+K^- pairs with KAOS/A1 is possible. With the beam energy being so close to threshold, the production of K^+K^- pairs will be dominated by intermediate ϕ meson production [16, 17]. Because of the small momentum of the ϕ ($\langle p \rangle \approx 800\,\mathrm{MeV}/c$) and in view of the small transverse momentum transfer, the two kaons are kinematically constrained and the relative azimuth angle of the two kaons peaks at 180°. The experiment will take advantage of this strong azimuthal correlation and of the large solid angle of KAOS/A1.

In order to explore the feasibility of a measurement of coherent ϕ production at the multi-spectrometer facility of MAMI, a schematic Monte Carlo study assuming coherent production on a deuterium nucleus was performed. In the left panel of Fig. 5 the momentum distribution of the produced ϕ mesons are presented which are detected within this set-up. As expected, the experimental conditions at MAMI-C allow the detection of ϕ mesons with rather low average momentum of approximately $0.75\,\mathrm{GeV}/c$. The right panel of Fig. 5 shows the reconstructed K^+K^- invariant mass. The two separated peaks correspond to ϕ decays inside (right) and outside (left) of the nucleus. The shift of the left peaks with respect to the free ϕ mass of $1.019\,\mathrm{GeV}/c^2$ reflects a bias caused by the finite momentum and angular acceptances for

the kaons. Comparing the dashed and solid histograms, one recognizes that by changing the positions of the two spectrometers the in-nucleus decays can be enhanced relative to decays outside of the nucleus.

6 Selection E: Two-Photon Exchange

Recently, the discussion about second-order processes in the electromagnetic interaction was nourished by the observation that the ratio of proton Sachs form factors, $R^2 = (\mu_p G_E^p / G_M^p)^2$, is different if measured by the method of Rosenbluth separation as compared to the extraction from the ratio of the transverse to longitudinal polarizations of the recoiling proton [18, 19]. A contribution from two-photon corrections was discussed as a possible explanation for this observation [20]. The two-photon contributions can be parameterized by the real part of the amplitudes $\hat{\mathrm{G}}_E$, $\hat{\mathrm{G}}_M$ and $\hat{\mathrm{F}}_3(s, Q^2)$, where these amplitudes are modifications of the usual Born approximation electromagnetic form factors.

The beam normal spin asymmetry $A_\perp$ is an asymmetry in the cross section for the elastic scattering of electrons with spin parallel ($\sigma_\uparrow$) and spin anti-parallel ($\sigma_\downarrow$) to the normal polarization vector. The evaluation of $A_\perp$ yields a dependence on the imaginary part of $\hat{\mathrm{F}}_3(s, Q^2)$. In contrast, the two-photon exchange contribution to the cross section is proportional to the real part of $\hat{\mathrm{F}}_3(s, Q^2)$. A direct ab initio calculation of the real part of $\hat{\mathrm{F}}_3(s, Q^2)$ does not seems to be feasible. It would involve the knowledge of the off-shell form factors of the proton in the intermediate state and also of all contributing excitations and their off-shell transition form factors.

The A4 collaboration has contributed to the study of the imaginary part of the two-photon exchange amplitude by a measurement of the beam normal spin asymmetry, $A_\perp$ [21]. The two lower panels of Fig. 6 show the results of measurements of $A_\perp$ with the forward angle set-up ($\theta_e \sim 30^\circ - 40^\circ$) for beam energies of 570 MeV and 854 MeV together with calculations by B. Pasquini. The upper panel contains new data at backward angles ($\theta_e \sim 140^\circ - 150^\circ$) for a beam energy of 315 MeV [1]. While the discrepancy between measured and calculated values of $A_\perp$ at forward angles could be explained by imperfect knowledge of higher mass intermediate states, the backward angle asymmetry should be dominated by the pure $\Delta(1232)$ excitation only. The exploration of $A_\perp$ by a series of measurements at different beam energies on proton and deuteron targets is foreseen at MAMI-C, and further studies of the induced recoil polarization, P_y, forbidden in one-photon exchange, are under consideration [1].

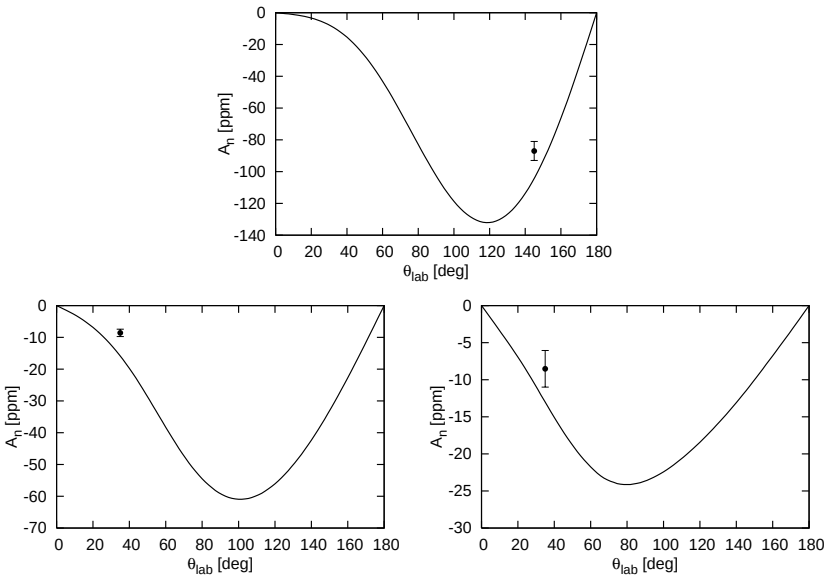

Figure 6: Results on $A_\perp$ at backward angles for a beam energy of 315 MeV (upper panel) [1] and forward angles for 510 MeV and 855 MeV (lower panels) [21]. The full line is a calculation by B. Pasquini.

7 The Physics Potential of MAMI-C

The commissioning of the new 1.5 GeV Harmonic Double-Sided Microtron as the fourth stage of MAMI is a great success in accelerator research and technology. Only a few selections from the wide range of the physics potential at MAMI-C could be presented in this paper. Embedded in the MAMI-C research profile, there are further programs for testing effective field theories, *e.g.* the study of the polarizability of the nucleon and the pion, and of generalized polarizabilities of the proton, programs for testing models of the NN interaction, reaction mechanisms and for models of nuclei, *e.g.* the study of few-body systems, and last but not least programs for studying the electromagnetic and strange form factors of the nucleon.

Acknowledgments

The physics program at MAMI is supported by the Deutsche Forschungsgemeinschaft (DFG) via the Sonderforschungsbereich SFB443 and the European Community Research Infrastructure Activity under the FP6 program HadronPhysics (RII3-CT-2004- 506078).

References

[1] *Funding proposal for Collaborative Research Centre 443: Many-body structure of strongly interacting systems*, Joh. Gutenberg-University (Mainz, 2007).

[2] A. Jankowiak, *Eur. Phys. J.* **A28**, sup. 1, 149 (2006).

[3] A. Bock *et al.*, *Phys. Rev. Lett.* **81**, 534 (1998).

[4] L. Tiator *et al.*, *Phys. Rev.* **C60**, 035210 (1999).

[5] H. Merkel *et al.*, *Phys. Rev. Lett.* **99**, 132301 (2007).

[6] W.-T. Chiang *et al.*, *Nucl. Phys.* **A700**, 429 (2002).

[7] H.-J. Arends, in *Proc. 9th Conf. on Intersections of Particle and Nuclear Physics*, *AIP Conf. Proc.* **870**, 481 (2006).

[8] P. Senger *et al.*, *Nucl. Inst. Meth. in Phys. Res.* **A327**, 393 (1993).

[9] P. Achenbach *et al.*, in *Proc. IX. Intern. Symp. on Detectors for Particle, Astroparticle and Synchrotron Radiation Experiments*, 144 (2006).

[10] A. I. Titov, M. Fujiwara and T.S.H. Lee, *Phys. Rev.* **C66**, 02202 (2002).

[11] H. W. Barz and M. Zétényi, *Phys. Rev.* **C69**, 024605 (2004).

[12] P. Mühlich *et al.*, *Phys. Rev.* **C67**, 024605 (2003).

[13] T. Hatsuda and S.H. Lee, *Phys. Rev.* **C46**, 34 (1992).

[14] F. Klingl, T. Waas and W. Weise, *Phys. Lett.* **B431**, 254 (1998).

[15] D. Cabrera and M.J. Vicente Vacas, *Phys. Rev.* **C69**, 065204 (2004).

[16] J. Barth *et al.*, *Eur. Phys. J.* **A17**, 269 (2003).

[17] A. Sibirtsev *et al.*, *Eur. Phys. J.* **A29**, 209 (2006).

[18] M. K. Jones *et al.*, *Phys. Rev. Lett.* **84**, 1398 (2000).

[19] O. Gayou *et al.*, *Phys. Rev. Lett.* **88**, 092301 (2002).

[20] P. A. M. Guichon and M. Vanderhaeghen, arXiv:hep-ph/0306007.

[21] F. Maas *et al.*, *Phys. Rev. Lett.* **94**, 152001 (2005).